The experimentally determined energy interval of 20 cm^{-1} in the ground state could, in principle, also result from spin-orbit effects instead of exchange interactions. We exclude this possibility on the basis of the observed polarization and temperature behavior of the 26 500-cm^{-1} band. Spin-orbit coupling would relax both the spin and the orbital selection rules, which are experimentally found to be strictly followed.

The fact that vivianite orders antiferromagnetically below 8.8 K[7] has not been taken into account in our discussion. With one exception, all oure measurements were done in the paramagnetic phase, where the dominant exchange effect is the ferromagnetic coupling of the two iron(II) centers within the dimers. From the crystal structure and the observed easy cleavage perpendicular to the *b* axis, some short-range magnetic order[13] within the *ac* plane extending to temperatures above the three-dimensional-ordering temperature cannot be ruled out. However, this order, if present, is antiferromagnetic and therefore cannot be responsible for the observed hot-band behavior.[14]

The sharp rise in intensity observed for several of the spin-forbidden transitions between liquid-helium temperature and 50 K is reminiscent of the behavior of spin-forbidden bands in the quasi-two-dimensional ferromagnet $FeCl_2$.[15] The hot absorption bands in $FeCl_2$ correspond to combined exciton-magnon excitations. This means that the intensity-gaining mechanism is essentially the same as the one postulated for vivianite, namely an exchange mechanism.[14] The main difference between the two systems is the collective character of the excitations in $FeCl_2$ as a result of the extended interactions in two dimensions, whereas in vivianite the excitations are localized on the ferromagnetically coupled dimers. The ferromagnetic sign of the exchange coupling in both systems is the result of a very similar (edge-sharing) bridging geometry.

Acknowledgment. This work was financially supported by the Swiss National Science Foundation under Grant No. 2.427-0.79.

Registry No. Vivianite, 14567-67-0.

(13) Carlin, R. L.; van Duyneveldt, A. J. "Magnetic Properties of Transition Metal Compounds"; Springer-Verlag: New York, 1977; p 142.

(14) Shinagawa, K.; Tanabe, Y. *J. Phys. Soc. Jpn.* **1971**, *30*, 1280.

(15) Robbins, D. J.; Day, P. *J. Phys. C* **1976**, *9*, 867.

Contribution from the Department of Chemistry, University of Utah, Salt Lake City, Utah 84112, and the Institut für Organische Chemie, Universität Heidelberg, D-6900 Heidelberg, West Germany

Preparation, Physical Nature, and Theoretical Studies of Tetrakis(3-methylpentadienyl)trimanganese, $Mn_3(3\text{-}CH_3C_5H_6)_4$[1]

MICHAEL C. BÖHM,[2a] RICHARD D. ERNST,*[2b] ROLF GLEITER,*[2a] and DAVID R. WILSON[2b,c]

Received October 26, 1982

The synthesis and characterization of tetrakis(3-methylpentadienyl)trimanganese are reported. Detailed X-ray structural data and variable-temperature magnetic susceptibility measurements support the formulation of this material as a high-spin Mn complex (five unpaired electrons) having a nearly linear trimetallic arrangement featuring an average Mn-Mn separation of 2.516 (1) Å and ∠Mn-Mn-Mn = 177.51 (6)°. The central manganese atom also interacts with one terminal carbon atom of each 3-methylpentadienyl ligand to achieve a nearly regular *edge*-bicapped tetrahedral coordination geometry (Mn-C = 2.331 (4) Å). The structure was refined to agreement indices $R = 0.050$, $R_w = 0.072$ in space group C_i^1-$P\bar{1}$ (No. 2) with $a = 6.937$ (1) Å, $b = 7.427$ (1) Å, $c = 23.940$ (3) Å, $\alpha = 83.54$ (1)°, $\beta = 83.77$ (1)°, and $\gamma = 64.15$ (1)°. Theoretical calculations using an INDO model have been carried out for doublet, quartet, and sextet states, with the result that the quartet is much higher in energy than the doublet or sextet configurations, which possess comparable energies. The central manganese atom appears to be attached to its nearest neighbors generally by only weak covalent couplings, although strong electrostatic influences appear to be present.

Introduction

Recently it has become clear that metal-pentadienyl compounds exhibit rich and diverse chemical features. In particular, a comparison of the pentadienyl anion with the related cyclopentadienyl and allyl anions has led to expectations of both stability and chemical reactivity in the open pentadienyl-metal systems. As a result, we have been vigorously pursuing a wide range of studies in order to gain a better understanding of these systems.[3] Of initial interest have been the bis(pentadienyl)metal compounds ("open metallocenes"), which have indeed demonstrated both stability and reactivity[3] and whose orbital bonding schemes have proven quite fascinating.[4] In the course of these studies, the very unusual complex $Mn_3(3\text{-}C_6H_9)_4$ ($3\text{-}C_6H_9$ = $3\text{-}CH_3C_5H_6$) was isolated from the reaction of $MnCl_2$ with 2 equiv of the 3-methylpentadienyl anion. Preliminary data suggested that this material could best be formulated as the associated salt $Mn^{2+}[Mn(3\text{-}C_6H_9)_2^-]_2$, in which the central manganese atom very nearly possessed a regular edge-bicapped tetrahedral coordination geometry.[5] Herein we report the results of complete spectroscopic, magnetic susceptibility, X-ray diffraction, and theoretical studies designed to more precisely define the nature of the compound.

Experimental Section

All operations involving organometallics were carried out under an atmosphere of prepurified nitrogen in Schlenk apparatus or in a glovebox. Nonaqueous solvents were thoroughly dried and deoxy-

(1) (a) Electronic structure of Organometallic Compounds. 23. See ref 1b for part 22. (b) Böhm, M. C.; Gleiter, R.; Berke, H. *J. Electron Spectrosc. Relat. Phenom.*, in press.

(2) (a) Universität Heidelberg. (b) University of Utah. (c) NSF Predoctoral Fellow, 1980-present.

(3) (a) Wilson, D. R.; DiLullo, A. A.; Ernst, R. D. *J. Am. Chem. Soc.* **1980**, *102*, 5928. (b) Wilson, D. R.; Ernst, R. D.; Cymbaluk, T. H., manuscript in preparation. (c) Wilson, D. R.; Liu, J.-Z.; Ernst, R. D. *J. Am. Chem. Soc.* **1982**, *104*, 1120. (d) Liu, J.-Z.; Ernst, R. D. *Ibid.* **1982**, *104*, 3737. (e) Ernst, R. D.; Cymbaluk, T. H. *Organometallics* **1982**, *1*, 708.

(4) Böhm, M. C.; Eckert-Maksić, M.; Ernst, R. D.; Wilson, D. R.; Gleiter, R. *J. Am. Chem. Soc.* **1982**, *104*, 2699.

(5) Wilson, D. R.; Liu, J.-Z.; Ernst, R. D. *J. Am. Chem. Soc.* **1982**, *104*, 1120.

0020-1669/83/1322-3815$01.50/0

genated in a manner appropriate to each and were distilled under nitrogen immediately prior to use. Elemental analyses were obtained from Galbraith Laboratories. 3-Methyl-1,3-pentadiene and 3-methyl-1,4-pentadiene were obtained from Wiley Laboratories and converted to the potassium salt of the 3-methylpentadienyl anion by a reported procedure.[6]

Spectroscopic Studies. Infrared spectra were recorded on a Perkin-Elmer Model 298 spectrophotometer. Mulls were prepared in a glovebox with dry, degassed Nujol. All infrared spectra were calibrated with polystyrene. Magnetic susceptibility measurements were carried out on a SHE VTS-50 susceptometer instrument. The sample was contained in a small aluminum capsule of known weight and magnetization as a function of temperature. A 5-kG field was employed for an 8.53-mg sample. A diamagnetic correction for the compound was estimated and applied.[7]

Tetrakis(3-methylpentadienyl)trimanganese, $Mn_3(3\text{-}C_6H_9)_4$. A magnetically stirred slurry of 0.50 g (4.0 mmol) of manganous chloride in 30 mL of THF was cooled to −78 °C under a N_2 atmosphere. To this was added dropwise 0.94 g (7.8 mmol) of the potassium salt of the 3-methylpentadienyl anion in 30 mL of THF. After slow warming to room temperature, the solvent was removed in vacuo, the product was extracted with hexane and the extractant was filtered through a medium frit. The microcrystalline product was isolated after cooling the concentrated solution to −78 °C. This product could be converted completely to homogeneous large single-crystal samples by slowly cooling concentrated solutions in hexane. Complete infrared data (Nujol mull): 1264 w, 1223 vs, 1188 s, 1143 s, 1120 w, 1030 ms, 988 vs, 975 sh, 922 w, 899 m, 889 sh, 880 sh, 864 sh, 831 m, 805 w, 768 m, 730 m cm^{-1}. A mass spectrum demonstrated the expected parent peak.

X-ray Diffraction Study of Tetrakis(3-methylpentadienyl)trimanganese. Well-formed single crystals of the compound could be obtained by bringing about slow cooling of a concentrated solution in hot hexane, which was accomplished by gradually decreasing the heat applied by a hot plate/oil bath combination. The amber platelike crystals were then loaded into and sealed within glass capillaries under a nitrogen atmosphere. Oscillation and Weissenberg photography revealed a triclinic unit cell that was confirmed by cell reduction procedures and later shown to be space group C_i^1-$P\bar{1}$ (No. 2). After the crystal was transferred to a Nicolet $P\bar{1}$ autodiffractometer, accurate cell constants and their standard deviations were derived from a least-squares refinement of 15 centered reflections for which $30° < 2\theta < 40°$, using the Mo K$\bar{\alpha}$ peak at 0.710 730 Å. The unit cell parameters are a = 6.937 (1) Å, b = 7.427 (1) Å, c = 23.940 (3) Å, α = 83.54 (1)°, β = 83.77 (1)°, γ = 64.15 (1)°, and V = 1100.4 (3) Å^3 for Z = 2 trimetallic units.

A general description of the equipment used has already been given.[8] Intensities were measured by using θ–2θ scans, which were from 1.4° below the Mo Kα_1 peak to 1.05° above the Mo Kα_2 peak. Data were collected in two concentric shells of 2θ, 0–40 and 40–50°, at respective scan rates of 2.4 and 1.7°/min with background time equaling 50% of the total scan time. The intensities of five standard reflections were monitored for every 95 reflections and evidenced no major decomposition. A total of 4096 reflections were collected, yielding 3888 unique reflections, of which 2431 had intensities deemed above background ($I > 3\sigma(I)$). These were utilized in subsequent calculations. The function minimized was $\sum w(|F_o| - |F_c|)^2$, with empirical weights assigned by the method of Cruikshank.[9] The atomic scattering factors were taken from a recent tabulation, as were the anomalous dispersion terms for manganese.[10] Calculations were undertaken with use of the X-RAY 70 programs as well as a modified version of the Ibers program AGNOST for absorption correction.[11]

Table I. Positional Coordinates for the Atoms of $Mn_3(3\text{-}CH_3C_5H_6)_4$

atom	x	y	z
Mn(1)	0.26447 (13)	0.04129 (11)	0.15233 (4)
Mn(2)	0.28112 (16)	0.13794 (14)	0.24853 (5)
Mn(3)	0.28236 (13)	0.23403 (12)	0.34589 (4)
C(1)	0.4656 (12)	0.1873 (11)	0.1269 (4)
C(2)	0.3637 (11)	0.1724 (9)	0.0814 (3)
C(3)	0.1423 (11)	0.2368 (8)	0.0786 (3)
C(4)	0.0014 (11)	0.2951 (9)	0.1265 (3)
C(5)	0.0482 (11)	0.3345 (9)	0.1795 (3)
C(6)	0.0592 (14)	0.2060 (11)	0.0267 (4)
C(7)	0.0678 (11)	−0.0930 (10)	0.1939 (3)
C(8)	0.1543 (11)	−0.1708 (9)	0.1408 (3)
C(9)	0.3764 (10)	−0.2524 (8)	0.1230 (3)
C(10)	0.5267 (10)	−0.2351 (8)	0.1542 (3)
C(11)	0.4921 (11)	−0.1695 (9)	0.2100 (3)
C(12)	0.4412 (13)	−0.3242 (10)	0.0647 (3)
C(13)	0.5491 (12)	−0.0506 (12)	0.3588 (5)
C(14)	0.4496 (13)	0.0349 (11)	0.4098 (4)
C(15)	0.2241 (13)	0.1013 (10)	0.4268 (4)
C(16)	0.0805 (12)	0.1219 (11)	0.3876 (3)
C(17)	0.1262 (12)	0.0499 (10)	0.3315 (3)
C(18)	0.1370 (18)	0.1920 (15)	0.4826 (4)
C(19)	0.0182 (12)	0.5018 (10)	0.3166 (3)
C(20)	0.1052 (12)	0.5338 (10)	0.3641 (4)
C(21)	0.3243 (13)	0.4865 (10)	0.3681 (4)
C(22)	0.4824 (12)	0.3755 (12)	0.3292 (4)
C(23)	0.4533 (12)	0.3203 (11)	0.2759 (3)
C(24)	0.3998 (16)	0.5167 (14)	0.4226 (4)

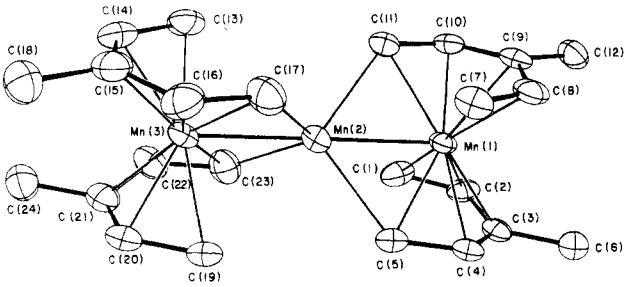

Figure 1. Perspective view of $Mn_3(3\text{-}C_6H_9)_4$. The hydrogen atoms have been deleted for clarity, and the 30% probability ellipsoids are shown.

The crystal faces were indexed as (001), (00$\bar{1}$), (101), ($\bar{1}$0$\bar{1}$), (010), (0$\bar{1}$0), and (120) for the crystal of approximate dimensions 0.1 × 0.4 × 0.8 mm. An absorption correction was applied (μ(Mo Kα) = 17.85 cm^{-1}) for which the transmission factors fell into the range 0.491–0.827. A Patterson map was used to provide trial positions for two independent manganese atoms. Several orientations were possible, but ensuing difference Fourier maps inevitably indicated the presence of at least one more heavy atom. Furthermore, it was noted that a linear trimetallic arrangement would actually fit the Patterson map much better, with all but one of the expected vectors appearing as the strongest peaks. Inclusion of such a unit, with anisotropic refinement, led to agreement indices[12] of R = 0.28 and R_w = 0.36. A difference Fourier map led to the location of all non-hydrogen atoms, which were also subjected to anisotropic refinement, leading to agreement indices R = 0.067 and R_w = 0.096. All hydrogen atoms were ultimately located and positioned in idealized locations (C–H = 0.95 Å). Isotropic thermal parameters were assigned for these atoms equal to 1.0 plus the equivalent isotopic thermal parameter for the atom to which they were attached. The final agreement indices were R = 0.050 and R_w = 0.072. A final difference Fourier map revealed no peaks greater than 0.33 e/Å^3. The standard deviation for the map was 0.07 e/Å^3. The final positional parameters for the non-hydrogen atoms obtained from the last cycle of least-squares refinement are presented in Table

(6) (a) Yasuda, H.; Ohnuma, Y.; Yamauchi, M.; Tani, H.; Nakamura, A. *Bull. Chem. Soc. Jpn.* **1979**, *52*, 2036. (b) Bates, R. B.; Gosselink, D. W.; Kaczynski, J. A. *Tetrahedron Lett.* **1967**, 199.

(7) (a) The estimated diamagnetic correction factor was 310 × 10^{-6} cgsu.[7b] (b) Mulay, C. N. In "Theory and Applications of Molecular Diamagnetism"; Mulay, L. N., Boudreaux, E. A., Eds.; Wiley-Interscience: New York, 1976.

(8) Neustadt, R. J.; Cymbaluk, T. H.; Ernst, R. D.; Cagle, F. W., Jr. *Inorg. Chem.* **1980**, *19*, 2375.

(9) (a) Cruikshank, D. W. J. In "Crystallographic Computing"; Ahmed, F. R., Ed.; Munksgaard: Copenhagen, 1970; pp 187–196. (b) The function applied in this case was $w = (100.0 + |F_o| + 0.10|F_o^2| + 0.007|F_o^3|)$.

(10) Cromer, D. T.; Waber, J. T. In "International Tables for X-ray Crystallography"; Kynoch Press: Birmingham, England, 1974; Vol. IV, Tables 2.2A and 2.3.1.

(11) (a) Stewart, J. A.; Kundell, F. A.; Baldwin, J. C. "The X-ray System of Crystallographic Programs"; Computer Science Center, University of Maryland: College Park, MD, 1970. (b) Ernst, R. D.; Marks, T. J.; Ibers, J. A. *J. Am. Chem. Soc.* **1977**, *99*, 2090.

(12) $R = \sum(|F_o| - |F_c|)/\sum F_o$; $R_w = [\sum w(|F_o| - |F_c|)^2/\sum wF_o^2]^{1/2}$.

Table IV. Selected Bond Distances (Å) and Angles (deg) in $Mn_3(3\text{-}C_6H_9)_4$

Bond Distances

		Mn(1)-Mn(2)	2.517 (2)	Mn(2)-Mn(3)	2.515 (2)		
Mn(1)-C(1)	2.116 (9)	Mn(1)-C(7)	2.124 (9)	Mn(3)-C(13)	2.133 (7)	Mn(3)-C(19)	2.143 (6)
Mn(1)-C(2)	2.065 (7)	Mn(1)-C(8)	2.082 (9)	Mn(3)-C(14)	2.062 (8)	Mn(3)-C(20)	2.091 (7)
Mn(1)-C(3)	2.148 (6)	Mn(1)-C(9)	2.146 (6)	Mn(3)-C(15)	2.153 (9)	Mn(3)-C(21)	2.148 (9)
Mn(1)-C(4)	2.061 (5)	Mn(1)-C(10)	2.065 (5)	Mn(3)-C(16)	2.045 (9)	Mn(3)-C(22)	2.060 (10)
Mn(1)-C(5)	2.162 (6)	Mn(1)-C(11)	2.163 (6)	Mn(3)-C(17)	2.154 (10)	Mn(3)-C(23)	2.148 (8)
Mn(2)-C(5)	2.335 (7)	Mn(2)-C(11)	2.340 (6)	Mn(2)-C(17)	2.321 (8)	Mn(2)-C(23)	2.339 (10)
C(1)-C(2)	1.400 (12)	C(7)-C(8)	1.416 (10)	C(13)-C(14)	1.407 (13)	C(19)-C(20)	1.431 (13)
C(2)-C(3)	1.402 (10)	C(8)-C(9)	1.423 (9)	C(14)-C(15)	1.446 (12)	C(20)-C(21)	1.415 (12)
C(3)-C(4)	1.398 (9)	C(9)-C(10)	1.404 (11)	C(15)-C(16)	1.391 (13)	C(21)-C(22)	1.382 (11)
C(4)-C(5)	1.436 (11)	C(10)-C(11)	1.432 (11)	C(16)-C(17)	1.452 (11)	C(22)-C(23)	1.444 (13)
C(3)-C(6)	1.505 (13)	C(9)-C(12)	1.501 (10)	C(15)-C(18)	1.507 (12)	C(21)-C(24)	1.532 (15)

Bond Angles

Mn(1)-Mn(2)-Mn(3)	177.51 (6)	C(11)-Mn(2)-C(17)	103.63 (25)	C(10)-C(9)-C(12)	119.8 (6)
Mn(1)-Mn(2)-C(5)	52.76 (17)	C(11)-Mn(2)-C(23)	118.35 (26)	C(13)-C(14)-C(15)	125.0 (9)
Mn(1)-Mn(2)-C(11)	52.73 (18)	C(17)-Mn(2)-C(23)	105.04 (30)	C(14)-C(15)-C(16)	119.9 (8)
Mn(1)-Mn(2)-C(17)	125.11 (24)	C(1)-C(2)-C(3)	126.3 (6)	C(15)-C(16)-C(17)	128.7 (7)
Mn(1)-Mn(2)-C(23)	129.84 (20)	C(2)-C(3)-C(4)	121.1 (7)	C(14)-C(15)-C(18)	119.8 (9)
Mn(3)-Mn(2)-C(5)	126.35 (17)	C(3)-C(4)-C(5)	126.9 (7)	C(16)-C(15)-C(18)	118.9 (7)
Mn(3)-Mn(2)-C(11)	128.04 (19)	C(2)-C(3)-C(6)	119.5 (6)	C(19)-C(20)-C(21)	124.9 (7)
Mn(3)-Mn(2)-C(17)	52.72 (23)	C(4)-C(3)-C(6)	118.4 (7)	C(20)-C(21)-C(22)	122.1 (9)
Mn(3)-Mn(2)-C(23)	52.38 (19)	C(7)-C(8)-C(9)	124.6 (7)	C(21)-C(22)-C(23)	127.4 (8)
C(5)-Mn(2)-C(11)	105.49 (26)	C(8)-C(9)-C(10)	121.4 (6)	C(20)-C(21)-C(24)	119.9 (7)
C(5)-Mn(2)-C(17)	116.67 (27)	C(9)-C(10)-C(11)	127.0 (6)	C(22)-C(21)-C(24)	116.6 (8)
C(5)-Mn(2)-C(23)	108.17 (28)	C(8)-C(9)-C(12)	118.0 (7)		

I, along with their estimated standard deviations. The remaining positional and thermal parameters are available as supplementary material (Tables II and III). The final values of the structure factor amplitudes are also available as supplementary material. Reflections for which the measured intensity was less than zero were assigned zero values of F_o. Other than those mentioned later, the intermolecular contacts were normal.

Results and Discussion

Synthetic and Structural Details. The reaction of $MnCl_2$ with 2 equiv of the 3-methylpentadienyl anion leads to the isolation of a brownish crystalline product, which differs noticeably from the presently known methylated bis(pentadienyl)metal complexes (metal = Ti, V, Cr, Fe, Ru). While the latter compounds are highly volatile and very hydrocarbon soluble, the manganese compound is much less hydrocarbon soluble and far less volatile. Initial analytical data were quite low in carbon and hydrogen for a formulation such as $Mn(3\text{-}C_6H_9)_2$, suggesting a more complex situation than had been expected and requiring a structural determination for resolution.

The result of the structural investigation is presented in Figure 1 along with the atom-numbering scheme. The stoichiometry is thus seen to be $Mn_3(3\text{-}C_6H_9)_4$ ($3\text{-}C_6H_9$ = $3\text{-}CH_3C_5H_6$). Pertinent bonding parameters may be found in Table IV. The three manganese atoms form a nearly linear array (∠Mn(1)–Mn(2)–Mn(3) = 177.51 (6)°), with the average Mn–Mn distance being 2.516 (1) Å. The coordination geometry of the two terminal manganese atoms is in some respects similar to that observed for iron in $Fe(2,4\text{-}C_7H_{11})_2$ ($2,4\text{-}C_7H_{11}$ = $2,4\text{-}(CH_3)_2C_5H_5$). Thus, the average Mn(1)– or Mn(3)–C bond distances are 2.129 (4), 2.075 (4), 2.149 (4), 2.058 (3), and 2.157 (4) Å, respectively, for the sequential carbon atoms C(1)–C(5) and their three equivalents. For the iron complex, the corresponding distances are 2.122 (3), 2.062 (3), 2.084 (3), 2.085 (4), and 2.095 (4) Å. The average Mn–C distance of 2.114 (2) Å is therefore seen to be slightly longer (by ca. 0.025 Å) than the average distance of 2.089 (1) Å in the iron complex. The difference is small enough compared to the usual magnitude of "electron imbalance" influences[13] to suggest that the terminal manganese atoms have no electron imbalance and therefore possess 18-electron configurations. The simplest formulation for the two terminal manganese atoms is therefore as the formally Mn(I) species $Mn(3\text{-}C_6H_9)_2^-$. This then necessitates the assignment of the central manganese atom as Mn(II), which would seem reasonable, but does not conform to the theoretical results (vide infra). The recent isolation of $Mn(C_5Me_5)_2^-$, however, lends support to this formulation.[14] There are, however, several differences between the geometries of $Mn(3\text{-}C_6H_9)_2^-$ and $Fe(2,4\text{-}C_7H_{11})_2$ that deserve note. First, the relative orientations of the pentadienyl ligands differ somewhat. One can define a conformation angle for a given complex as the angle between two ligand-related planes, each composed of the metal atom and two points derived for each given ligand—the C(3) atom and the midpoint between the C(1) and C(5) atoms. A cis-eclipsed ligand conformation will be assigned a conformation angle of 0°, while a trans-eclipsed will be 180°. Under this definition, the iron complex has a conformation angle of 59.7°, essentially identical with the idealized 60° for the gauche-eclipsed conformation (I).

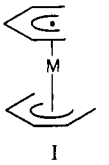

I

The terminal manganese species, however, are characterized by an average conformation angle of 35.6°, much closer to a staggered orientation. The obvious origin of this difference is the general nature of the pentadienyl ligands as well as the presence of the central manganese atom. The large size of the pentadienyl ligands tends to greatly clog a metal's coordination sphere, particularly since its large girth necessitates a close proximity of the metal atom to the ligand plane. In fact, the ligands become so close that substantially greater interligand C--C nonbonded contacts are experienced as compared to those of cyclopentadienyl systems. For this reason, the classic bent metallocene sandwich configurations[15]

(13) Haaland, A. *Acc. Chem. Res.* **1979**, *12*, 415.

(14) Robbins, J. L.; Edelstein, N. M.; Cooper, S. R.; Smart, J. C. *J. Am. Chem. Soc.* **1979**, *101*, 3853.

would not seem to have an analogue in at least the smaller transition-metal bis(pentadienyl) systems. Instead, the two pentadienyl ligands remain essentially parallel (6.3° for Mn-$(3\text{-}C_6H_9)_2^-$ vs. 15.0° for Fe$(2,4\text{-}C_7H_{11})_2$ but twist toward the cis-eclipsed conformation to allow placement of a third ligand by the open edge of the pentadienyl ligands, e.g., II.

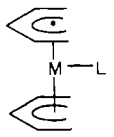

II

In the present compound, L is actually the central manganese atom, formally Mn(II). Besides its nearly linear interaction with the two terminal manganese atoms, this species should certainly prefer to engage in further interactions, which are brought about by the twisting of the 3-methylpentadienyl ligands from the cis-eclipsed configuration (0°) to the observed 35.6°. It can readily be seen that this twisting brings one terminal pentadienyl carbon atom into the proximity of the central manganese atom. The resulting Mn(2)–C(bridge) distances average 2.331 (4) Å, and the disposition of these four carbon atoms around Mn(2) is seen (Table IV) to be very nearly tetrahedral. The overall coordination sphere of the central Mn(2) atom then is best described as *edge*-bicapped tetrahedral. Such a bizarre coordination geometry precludes a formulation for the central Mn(2) atom as anything related to a usual 16- or 18-electron bonding pattern but would be quite reasonable for a more ionic species, such as a classic high-spin Mn(II) ion.[16] Indeed, this picture was consistent with preliminary magnetic susceptibility data,[5] and the overall complex may be formulated as an associated salt, Mn^{2+}-$[Mn(3\text{-}C_6H_9)_2^-]_2$. The distances between the central manganese atom and the other (further) terminal carbon atoms are 3.100 (8), 3.160 (9), 3.216 (10), and 3.055 (7) Å. The interaction of the apparent electrophile Mn^{2+} with both the metal and carbon atoms of the terminal $Mn(3\text{-}C_6H_9)_2$ anions provides clear evidence of both metal and ligand basicities in these open systems, and the partial interaction of the central Mn^{2+} with each may actually bear a relationship to the course of electrophilic substitution reactions in ferrocene-like molecules. It seems worthy to speculate that other related associated salts should also be preparable by the interaction of $MnCl_2$ with various organometallic anions.

Before turning to ligand-related parameters, it is perhaps useful to attempt to assess the importance of the interaction between the central Mn(2) atom and the terminal pentadienyl carbon atoms with which it interacts. Since the C(5) atom and its equivalents are also bound to the C(4) atom and a terminal manganese atom, substantial Mn(2)–C5 interaction should lead to a weakening of the C4–C5 and Mn(1)– or Mn(3)–C5 bonds. (The use of C5 rather than C(5) here is meant to indicate that the corresponding distances involving the related atoms C(11), C(17), and C(23) are also being included to give an average value here.) Indeed, the C4–C5 bond distances are significantly longer than the rest, averaging 1.441 (6) Å compared to the other inner-ligand C–C distances that average 1.410 (3) Å. Further, the Mn(1)– or Mn(3)–C5 distance is longer than the average Mn(1)– or Mn(3)–C1 distance (2.157 (4) vs. 2.129 (4) Å), whereas in the Fe-$(2,4\text{-}C_7H_{11})_2$ structure the opposite ordering is observed (2.095 (4) vs. 2.122 (3) Å). Thus, the interaction of the central manganese atom with the terminal manganese atoms and the bridging carbon atoms does appear to be substantial enough to bring about a noticeable weakening of the proximate bonds present within the $Mn(3\text{-}C_6H_9)_2^-$ portions.

The ligands themselves are nearly planar. However, there are consistent deviations that are −0.01 Å (1, 5 positions), 0.04 Å (2,4 positions), and −0.05 Å (3 positions), where a positive deviation indicates a deformation toward the manganese atom. The methyl carbon atoms are bent toward the manganese atoms by an average 3.7° (0.047 Å below the ligand planes). The hydrogen atoms attached to the C2 and C4 atoms are also located out of the ligand plane by an average of 0.14 Å toward their respective manganese atoms. Similar substituent tilts toward the metal atom have also been observed for ferrocene (3.7 (9)°) and attributed to an attempt by the ligand to direct its p orbitals more toward the iron atom.[13] The apparently larger (on the average) pentadienyl tilts here can be ascribed to the greater size of the ligand, which presumably would result in poorer overlap. A related twisting distortion is also observed for the terminal CH_2 groups. The exo H atoms are located ca. 0.28 Å out of their ligand planes in a direction toward the manganese atom, presumably in part for the same reason as above. However, the endo hydrogen atoms are located ca. 0.72 Å out of the ligand plane in a direction away from the manganese atoms. The much larger magnitude of this displacement might suggest that this distortion is due more to intra-

Table V. Magnetic Susceptibility Data for $Mn_3(3\text{-}C_6H_9)_4$[a]

T, K	χ_{cor}, cgsu	$1/\chi_{cor}$, $cgsu^{-1}$	μ_{eff}, μ_B
2.17	1.750 3	0.57133	5.51
3.01	1.297 8	0.77053	5.59
5.06	0.787 3	1.2702	5.65
6.00	0.669 9	1.4928	5.67
10.00	0.401 2	2.4925	5.67
15.00	0.268 4	3.7258	5.68
20.00	0.202 0	4.9505	5.69
30.00	0.135 5	7.3801	5.70
40.00	0.102 0	9.8039	5.71
50.00	0.082 03	12.191	5.73
65.00	0.063 46	15.758	5.74
80.00	0.051 08	19.577	5.72
100.5	0.039 49	25.323	5.63
120.0	0.033 93	29.472	5.71
140.2	0.029 08	34.388	5.71
160.2	0.026 15	38.241	5.79
181.8	0.023 19	43.122	5.81
200.0	0.020 32	49.213	5.70
225.0	0.018 04	55.432	5.70
250.0	0.016 43	60.864	5.73
275.0	0.014 92	64.024	5.73
300.0	0.013 99	71.480	5.79

[a] Curie behavior is assumed in these calculations.

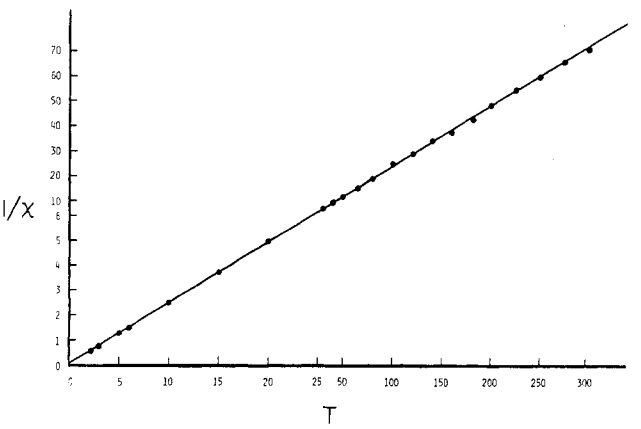

Figure 2. Plot of the reciprocal magnetic susceptibility of $Mn_3(3\text{-}C_6H_9)_4$ as a function of temperature (K). A change in scale occurs at 25 K.

(15) Lauher, J. W.; Hoffmann, R. *J. Am. Chem. Soc.* **1976**, *98*, 1729 and references therein.
(16) (a) Cotton, F. A.; Wilkinson, G. "Advanced Inorganic Chemistry", 4th ed.; Interscience: New York, 1980. (b) Bünder, W.; Weiss, E. *Z. Naturforsch., B: Anorg. Chem., Org. Chem.* **1978**, *33B*, 1235.

Table VI. Relative Energies ΔE (kJ/mol) of Tetrakis(pentadienyl)trimanganese in the Doublet, Quartet, and High-Spin Sextet States according to the Semiempirical INDO MO Approach

	doublet	quartet	sextet
ΔE	0.0	124.8	0.8

ligand H_{endo}--H_{endo} repulsions than to ligand attempts to improve overlap with the manganese atoms.

Magnetic Susceptibility Measurements. The magnetic data are given in Table V. A plot of $1/\chi$ vs. T is presented in Figure 2. It is quite clear that Curie–Weiss behavior is observed over the range 2.17–300 K.[17] The average value of μ_{eff} is 5.70 μ_B, while that derived from the slope of the least-squares line (Figure 2) is 5.75 μ_B.[17] These values are quite comparable to the spin moment expected for a five-unpaired-electron system, 5.92 μ_B, and are consistent with the formulation of this compound as the associated salt of the high-spin (ionic) Mn^{2+} and the diamagnetic, 18-electron $Mn(3\text{-}C_6H_9)_2^-$, as well as the formulation as a high-spin sextet, described in the following section.

Theoretical Studies. The electronic structure of the title compound has been investigated by means of a recently developed semiempirical INDO model.[18] The ZDO operator has been designed to reproduce computational results of double-ζ ab initio calculations. The method has been successfully used to study the ground-state and cationic hole-state properties of metallocenes[19] and open metallocenes[4] as well as the electronic structure of weakly coupled bi- and polynuclear transition-metal complexes.[20-24] Therefore, it can be expected that the present results are also of reliable quality. We have adopted the experimental structural parameters of the aforementioned X-ray investigation; the methyl groups in the pentadienyl ligands, however, have been replaced by hydrogen atoms. The following open-shell configurations of the polynuclear Mn complex have been considered: a doublet state with one unpaired electron, a quartet configuration with three unpaired electrons, and a high-spin sextet. We have employed a UHF open-shell formalism[25] for the INDO calculations. The MO calculations have been performed without spin projection. The large molecular dimensions prevent the application of sophisticated extended projection techniques, and simplified methods based on a single annihilator gave discouraging results in the case of semiempirical MO methods that are based on the ZDO approximation.[26] The serious shortcomings of the latter method are especially well documented in the case of transition-metal complexes.[27] For a critical comparison of the relative energies for the three open-shell configurations

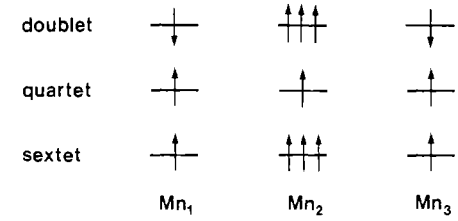

Figure 3. Simplified picture of the spin structure in the doublet, quartet, and sextet configurations of I.

it must be mentioned, however, that the UHF determinants contain admixtures from higher spin states; these contributions are of larger significance in the low-spin (doublet) configuration compared to those in the quartet and sextet states.

The relative energies for the three spin states of the title compound are summarized in Table VI. It is seen that the doublet and sextet states have identical energies within the accuracy of a semiempirical MO approach; the quartet state on the other hand is high above the doublet and sextet states. While the magnetic measurements reveal that the high-spin sextet corresponds to the electronic ground state of the trinuclear Mn complex, the INDO MO calculations suggest the possibility of a high-spin–low-spin equilibrium, a situation that is well-known in the chemistry of manganese complexes.[13,16]

In order to understand the differences in the doublet–quartet–sextet series, we have summarized the calculated net charges, spin densities, and net populations[28] for the α- and β-spin electrons in Table VII. The coordinate system is given as follows:

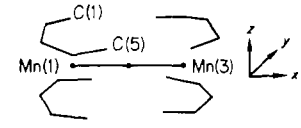

The INDO MO data demonstrate that the electronic (spin) structures at the central transition-metal atom are nearly identical in the doublet and sextet states. The electronic configuration at Mn(2) in both spin states is characterized by three unpaired electrons. The spin structure in the doublet state requires two electrons with opposite spins at the terminal manganese sites while two α-spin electrons at Mn(1) and Mn(3) lead to the high-spin sextet. The electronic structure of the quartet differs significantly from the electronic population in the low- and high-spin configurations. Each atom contributes one unpaired electron to the net spin state of the compound; the necessary condition for this behavior is a pronounced electron redistribution at the central manganese atom. A simplified display of the spin structure in the three open-shell systems is given in Figure 3. The nature of the metal–metal coupling in the doublet is of antiferromagnetic character (alternating β–α–β spins) while the two remaining states are coupled ferromagnetically. The equivalence of the electronic structures at Mn(2) in the doublet and sextet is clearly seen. Both states can be easily interconverted by a two-spin flip ($\beta \rightleftarrows \alpha$) at the terminal Mn centers. The results of Table VII furthermore demonstrate that the spin density at Mn(1)/Mn(3) leads to a pronounced spin polarization in the pentadienyl ligands. This polarization is most efficient in the case of the two carbon atoms that are rotated into the direction of the transition-metal centers.

The individual AO and spin populations at the 3d centers are summarized in Table VIII. The computational results clearly indicate that the foregoing discussion of the electronic structure at the transition-metal centers is only a simplified

(17) (a) From a least-squares fit of the data in Table V to a straight line ($1/\chi$ vs. T), a value of $\Theta = -0.60$ K results ($\chi = C(T - \Theta)^{-1}$).[17d] χ here represents the molar susceptibility. (b) The value of 5.70 μ_B is an average of all values presented in the table, each value being determined through $\mu_{eff} = (8\chi_{cor}T)^{1/2}$. These values were derived by assuming Curie behavior. If Curie–Weiss behavior is assumed, the average becomes 5.81 μ_B. (c) The value of 5.70 μ_B was derived from the slope of the line in Figure 2 by using the relationship $1/\chi_{cor} = (T - \Theta)(3k/N\beta^2\mu_{eff}^2)$. (d) See: "Theory and Applications of Molecular Paramagnetism"; Boudreaux, E. A., Mulay, L. N., Eds.; Wiley-Interscience: New York, 1976.

(18) Böhm, M. C.; Gleiter, R. *Theor. Chim. Acta.* **1981**, *59*, 127, 153.
(19) Böhm, M. C. *Z. Naturforsch. A* **1982**, *37A*, 1193.
(20) Böhm, M. C.; Gleiter, R.; Delgado-Pena, F.; Cowan, D. O. *Inorg. Chem.* **1980**, *19*, 1081. Böhm, M. C.; Gleiter, R.; Delgado-Pena, F.; Cowan, D. O. *J. Chem. Phys.*, in press.
(21) Böhm, M. C.; Gleiter, R. *Chem. Phys.* **1982**, *64*, 183. Böhm, M. C.; *Ber. Bunsenges, Phys. Chem.* **1982**, *86*, 56. Böhm, M. C. *Theor. Chim. Acta* **1982**, *60*, 455.
(22) Böhm, M. C. *Ber. Bunsenges. Phys. Chem.* **1981**, *85*, 755.
(23) Böhm, M. C. *Theor. Chim. Acta* **1981**, *60*, 233.
(24) Böhm, M. C. *Mol. Phys.* **1982**, *46*, 683.
(25) Slater, J. C. *Phys. Rev.* **1930**, *35*, 210. Pople, J. A.; Nesbet, R. K. *J. Chem. Phys.* **1954**, *22*, 571.
(26) Beveridge, D. L.; Dobosh, P. A. *J. Chem. Phys.* **1968**, *48*, 5532. Bischof, P. *J. Am. Chem. Soc.* **1976**, *98*, 6844.
(27) Brown, R. D.; Burton, P. G. *Theor. Chim. Acta* **1970**, *18*, 309. Bacon, A. D. Zerner, M. C. *Theor. Chim. Acta* **1979**, *53*, 21.
(28) Mulliken, R. S. *J. Chem. Phys.* **1955**, *23*, 1833, 2343.

Table VII. Net Charges (q_i), Spin Densities (ρ_i), and Net Populations for α- and β-Spin Electrons (n_α and n_β) in Tetrakis(pentadienyl)trimanganese in the Doublet, Quartet, and Sextet States according to the Semiempirical INDO MO Approach

	q_i			ρ_i			n_α			n_β		
atom	doublet	quartet	sextet	doublet	quartet	sextet	doublet	quartet	sextet	doublet	quartet	sextet
Mn(1)-Mn(3)	0.258	0.249	0.249	−1.072	1.057	1.059	2.835	3.904	3.905	3.907	2.847	2.846
Mn(2)	−0.221	−0.196	−0.163	1.900	1.105	3.040	5.061	4.163	5.102	2.161	3.058	2.062
C(1)	−0.477	−0.482	−0.480	0.284	−0.226	−0.229	2.381	2.128	2.126	2.097	2.354	2.355
C(2)	0.015	0.024	0.023	−0.023	0.010	0.009	1.978	1.998	1.993	2.008	1.988	1.984
C(3)	−0.232	−0.239	−0.240	−0.043	0.032	0.038	2.095	2.136	2.139	2.138	2.104	2.101
C(4)	0.005	0.014	0.022	0.236	−0.180	−0.180	2.111	1.903	1.899	1.875	2.083	2.079
C(5)	−0.412	−0.417	−0.432	−0.402	0.340	0.326	2.005	2.379	2.379	2.407	2.039	2.053

Table VIII. AO Populations and AO Spin Densities at the Transition-Metal Centers of Tetrakis(pentadienyl)trimanganese in the Doublet, Quartet, and Sextet States according to the INDO Formalism

		AO population			AO spin density		
atom	AO	doublet	quartet	sextet	doublet	quartet	sextet
Mn(1)	4s	0.1105	0.1106	0.1108	−0.0014	0.0012	0.0012
Mn(3)	$4p_x$	0.0764	0.0764	0.7666	−0.0009	0.0012	0.0011
	$4p_y$	0.0807	0.0807	0.0807	−0.0012	0.0013	0.0013
	$4p_z$	0.0838	0.0839	0.0838	−0.0007	0.0006	0.0006
	$3d_{z^2}$	1.9203	1.9507	1.9362	−0.0695	0.0393	0.0542
	$3d_{xz}$	0.9538	0.9612	0.9576	−0.0983	0.1239	0.1212
	$3d_{yz}$	0.8229	0.8150	0.8174	−0.1528	0.1371	0.1373
	$3d_{x^2-y^2}$	1.0772	1.0552	1.0816	−0.7219	0.7465	0.7233
	$3d_{xy}$	1.6166	1.6175	1.6063	−0.0025	0.0062	0.0189
Mn(2)	4s	0.0852	0.0854	0.0859	−0.0002	0.0020	0.0020
	$4p_x$	0.0706	0.0708	0.0708	−0.0006	0.0006	0.0013
	$4p_y$	0.0533	0.0533	0.0534	0.0013	0.0003	0.0009
	$4p_z$	0.0606	0.0606	0.0604	0.0011	−0.0001	0.0007
	$3d_{z^2}$	1.6870	1.0068	1.4486	0.2933	0.1727	0.5424
	$3d_{xz}$	1.0125	1.0167	1.0181	0.9469	0.9456	0.9527
	$3d_{yz}$	1.0013	1.9561	1.9417	0.9744	0.0226	0.0419
	$3d_{x^2-y^2}$	1.2967	0.9900	1.4789	0.6886	−0.1513	0.5198
	$3d_{xy}$	1.9539	1.9560	1.0056	−0.0061	0.0123	0.9775

description of the "true" electron configurations. The AO populations at Mn(1)/Mn(3) in the doublet, quartet, and sextet show the following identical gradation:

Mn(1)/Mn(3)

doublet, quartet, sextet: $3d_{z^2} > 3d_{xy} > 3d_{x^2-y^2} > 3d_{xz} > 3d_{yz}$

The distribution scheme at the central Mn atom on the other hand differs significantly:

Mn(2)

doublet: $3d_{xy} > 3d_{z^2} > 3d_{x^2-y^2} > 3d_{xy}, 3d_{yz}$
quartet: $3d_{yz}, 3d_{xz} > 3d_{z^2}, 3d_{xz}, 3d_{x^2-y^2}$
sextet: $3d_{yz} > 3d_{x^2-y^2}, 3d_{z^2} > 3d_{xz}, 3d_{yz}$

The doublet and quartet configurations at Mn(2) differ primarily in the populations of the $3d_{z^2}$ and $3d_{yz}$ orbitals, the latter being more highly populated in the higher spin state. The occupation in $3d_{yz}$ is conserved in the sextet; additionally a transfer from $3d_{xy}$ into $3d_{x^2-y^2}$ and $3d_{z^2}$ is diagnosed.

Wiberg bond indices[29] for the three possible open-shell configurations are compared in Figure 4. The covalent interaction between the 3d centers is weak irrespective of the specific spin configuration at the transition-metal atoms. The net charges in Table VII thus suggest that the Mn/Mn potential is mainly determined by electrostatic forces between the positively charged terminal sides and the central Mn atom with a surplus of negative charge. A second important interaction that stabilizes the trinuclear complex is the interaction between one terminal carbon atom of the organic ligand and the central manganese atom. It is this covalent coupling

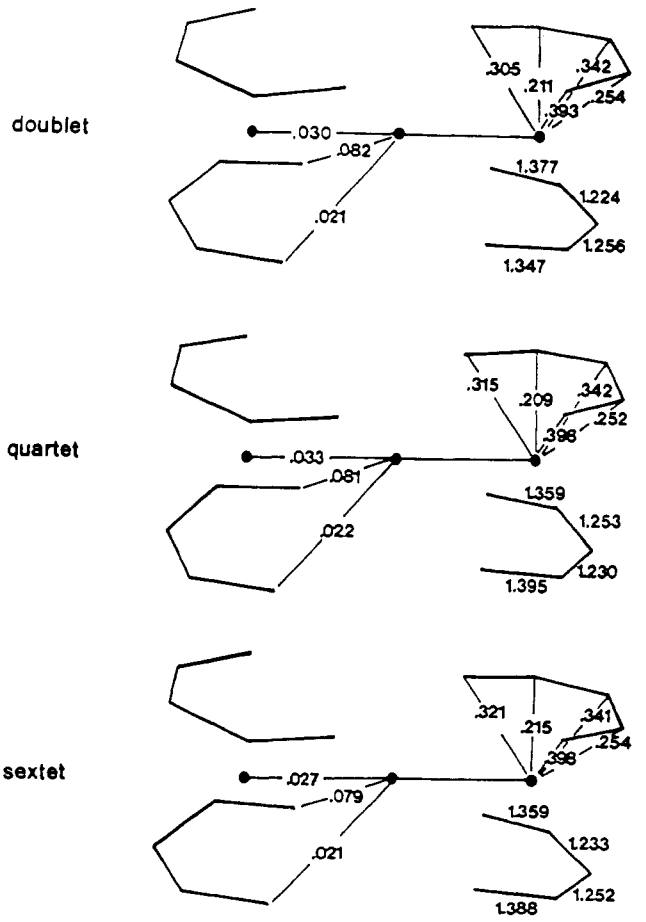

Figure 4. Wiberg bond indices of the doublet, quartet, and sextet configurations of I.

(29) Wiberg, K. B. *Tetrahedron* **1968**, *24*, 1083.

that is responsible for the edge-bicapped tetrahedral coordination of Mn(2) in the trinuclear complex. A similar interaction pattern has been detected in some lithium-coordinated transition-metal derivatives.[30] The bond indices between the terminal manganese centers and the carbon atoms in the organic frameworks are comparable with the Wiberg indices found for the open ferrocenes.[4] This is also true for the slight alternancy in the pentadienyl carbon framework.

Concluding Remarks. The data described herein provide some interesting contrasts and comparisons between the original compound formulation of $Mn^{2+}[Mn(3\text{-}C_6H_9)_4]^-$ and the more sophisticated description developed by the theoretical studies, particularly with respect to placement of electrons and net charges. Nevertheless, both sets of results are reasonably consistent with one another in terms of total unpaired electrons in the ground state and the weak covalent bonding interactions expected between the central manganese atom and the nearby atoms in its *edge*-bicapped tetrahedral geometry. To some extent the difference between the two models may be related to the situation for metal hydrides, where the hydrogen atom may behave more as an acid or as a hydride depending on circumstance. In either case, the same metal and hydrogen orbitals are involved, and the actual charges are dependent on the relative proportions of the metal and hydrogen orbitals contributing to the ground state orbital. Thus, the simple ionic formulation and the more sophisticated theoretical sextet model may really bear some resemblance to one another after all. Further efforts to gain a better understanding of this system are in progress.

Acknowledgment. The work at Heidelberg has been supported by the Fonds der Chemischen Industrie, the Stiftung Volkswagenwerk, and the BASF Aktiengesellschaft in Ludwigshafen. The work at Utah has been supported by the National Science Foundation (Grant No. CHE-8120683), the donors of the Petroleum Research Fund, administered by the American Chemical Society, and the University of Utah Research Committee. R.G. and R.D.E. are further grateful to NATO for a travel grant, without which the pursuit of these studies would have been much more difficult. We thank Prof. Tobin Marks and Dr. Tamotsu Inabe of Northwestern University for helping us obtain the magnetic measurements.

Registry No. $Mn_3(3\text{-}CH_3C_5H_6)_4$, 85976-94-9; $MnCl_2$, 7773-01-5; Mn, 7439-96-5; potassium 3-methylpentadienyl, 74206-00-1.

Supplementary Material Available: A listing of observed and calculated structure factor amplitudes and Tables II and III, showing non-hydrogen atom thermal parameters and hydrogen atom positional and thermal parameters (22 pages). Ordering information is given on any current masthead page.

(30) Böhm, M. C.; Gleiter, R. *J. Organomet. Chem.* **1982**, *228*, 1.

Contribution from the Department of Hydrocarbon Chemistry, Faculty of Engineering, Kyoto University, Kyoto 606, Japan

ESR Study of the Electronic Structure of $Co_3(\eta^5\text{-}C_5H_5)_3(\mu_3\text{-}CPh)_2$

SACHIO ENOKI, TAKASHI KAWAMURA,* and TEIJIRO YONEZAWA

Received April 7, 1983

The anion and cation radicals of $Co_3(\eta^5\text{-}C_5H_5)_3(\mu_3\text{-}CPh)_2$ are generated by reduction with potassium metal and by electrochemical oxidation, respectively. The frozen-solution ESR spectra of the anion show the Co_3 triangle to be regular. Its odd electron is accommodated in the a_2' MO (D_{3h} point group) constructed mainly from cobalt d AO's, and the odd-electron density on the cobalt d AO is estimated as 0.18. The ESR spectrum of the cation suggests that the odd-electron orbital is a degenerate one. An MO diagram constructed by using the method of Dahl and co-workers is consistent with the present ESR results. The odd-electron distribution in the present anion radical is compared with those of closely related $Co_3(CO)_9(\mu_3\text{-}CPh)^{-\cdot}$ and $Co_3(CO)_9S\cdot$.

Elucidation of electronic structures and assignment of frontier orbitals of triangular M_3 clusters with μ_3 ligand(s) are being developed by Dahl and co-workers by analyses of geometrical deformations caused by changes in the number of valence electrons[1] and by an ESR study of $Co_3(CO)_9S\cdot$[2] (**1**),

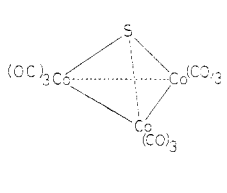

1

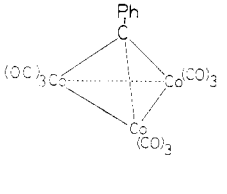

2

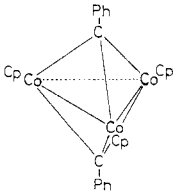

3

Cp = C_5H_5

which is isoelectronic to $Co_3(CO)_9(\mu_3\text{-}CPh)^{-\cdot}$ (**2**$^-$). The latter tricobalt complex has been examined by Robinson and his colleagues.[3] ESR studies of ion radicals of metal clusters with higher geometrical symmetries are expected to reveal electronic characteristics complementary to those obtained by studies of geometrical effects.

Herein is presented our ESR study of ion radicals derived from $Co_3(\eta^5\text{-}C_5H_5)_3(\mu_3\text{-}CPh)_2$ (**3**), which has a pseudo-D_{3h} geometry.[4] Our results fully support the method of constructing a qualitative molecular orbital (MO) diagram to reproduce frontier orbitals developed by Dahl and co-workers.[2,5] The d character of the odd-electron orbital of **3**$^-$ is

(1) (a) Mag, J. J.; Ral, A. D.; Dahl, L. F. *J. Am. Chem. Soc.* **1981**, *104*, 3054 and references cited therein. (b) See also: Schilling, B. E. R.; Hoffmann, R. *Ibid.* **1979**, *101*, 3456.
(2) Strouse, C. E.; Dahl, L. F. *Discuss. Faraday Soc.* **1969**, *47*, 93; *J. Am. Chem. Soc.* **1971**, *93*, 6032.
(3) Peake, B. M.; Rieger, P. M.; Robinson, B. H.; Simpson, J. *Inorg. Chem.* **1979**, *18*, 1000.
(4) The trigonal-bipyramidal core of $Co_3(\eta^5\text{-}C_5H_5)_3(\mu_3\text{-}CSiMe_3)(\mu_3\text{-}C_3SiMe_3)$ has a pseudo-D_{3h} geometry: Fritch, J. R.; Vollhardt, K. P. C.; Thompson, M. R.; Day, V. W. *J. Am. Chem. Soc.* **1979**, *101*, 2768.
(5) Vahrenkamp, H.; Uchtman, V. A.; Dahl, L. F. *J. Am. Chem. Soc.* **1968**, *90*, 3272.

0020-1669/83/1322-3821$01.50/0